ISSN 0001-4338, Izvestiya, Atmospheric and Oceanic Physics, 2021, Vol. 57, No. 12, pp. 1566–1575. © Pleiades Publishing, Ltd., 2021.
Russian Text © The Author(s), 2021, published in Issledovanie Zemli iz Kosmosa, 2021, No. 4, pp. 84–96.

METHODS AND TOOLS FOR PROCESSING AND INTERPRETING SPACE INFORMATION

Spatiotemporal Spectral-Response Assessment of the Forest Cover of Small Dry Valleys in the Central Russian Forest–Steppe

E. A. Terekhin*

Federal Regional Centre of Aerospace and Ground Monitoring of Objects and Natural Resources, Belgorod State University, Belgorod, 308015 Russia

**e-mail: terekhin@bsu.edu.ru*

Received February 9, 2021; revised April 16, 2021; accepted June 4, 2021

Abstract—Results of assessment are presented for the relationship between the forest cover of small dry valleys and their spectral response through analysis of object data in the forest–steppe natural zone of the Central Chernozem region of Russia. The SWIR reflectance of small dry valleys is shown to be tightly correlated with the percentage of forest cover. The greater the forest cover, the lower the SWIR reflectance. A logistical dependence can be used to obtain spectral-response estimates for forest cover in the SWIR range. Spectral-response estimates are found for the forest cover of small dry valleys in the Central Russian forest steppe from *Landsat* data in the mid-1980s, early 2000s, and late 2010s. Recent decades have seen an increase in the forest-cover percentage of small dry valleys throughout most of the region. From the mid-1980s to 2018, the forest cover increased from 16 to 45%. During the study period, an increase is observed in intraregional differences in the forest cover of ravines. Currently, this indicator varies more significantly within the region than in the mid-1980s.

Keywords: small dry valleys, forest cover, Central Russian forest–steppe, remote sensing data, spectral response, *Landsat*

DOI: 10.1134/S0001433821120215

INTRODUCTION

Small dry valleys are a characteristic component of the Central Russian forest–steppe landscapes within the Central Chernozem region (Mil'kov et al., 1978; Nechetova and Narozhnyaya, 2010). Small dry valleys are one of the few natural-landscape elements that can help researchers identify regional trends in vegetation cover. This is due to the degree of anthropogenic transformation throughout most of the region and the intensive agricultural use of the land. Changes in the vegetation cover of small dry valleys (SDVs), primarily those related to the forest-cover percentage, can serve as an indicator of modern trends in the development of natural vegetation.

At the beginning of the 20th century, the forest cover of the Central Chernozem region (CCR) was about 8.7% (Bugaev et al., 2006). In recent decades, some growth has been recorded in the south of the Central Russian Upland (on the territory of the Belgorod oblast), mainly due to the SDV network (Terekhin and Chendev, 2018). Given the high anthropogenic load on most of the regional landscapes, SDVs are one of the few factors that enable a natural increase in forest cover (Chendev et al., 2016). Forest-cover indicators can determine microclimatic (Ol'chev et al., 2017; Bonan, 2008; Gao, 2012) and hydrological conditions (Onuchin et al., 2017) and affect the appearance of the landscape. For this reason, it is currently relevant to conduct a modern and retrospective assessment of the SDV forest cover in the CCR forest–steppe zone. A study of modern trends in the development of SDV vegetation cover is relevant also because of the ongoing climatic changes in the CCR (Lebedeva and Krymskaya, 2008; Novikova et al., 2017), which may be one of the reasons for the changes in natural vegetation.

Modern and archival satellite information is one of the most effective resources for spatiotemporal analysis of forested lands (Pis'man et al., 2018; Kozoderov et al., 2018; Kashnitskii et al., 2019; Terekhin, 2020). The use of satellite data allows retrospective estimates of forest cover (Kim et al., 2014; Belyaeva and Popov, 2016) and can be used to assess features of forest-vegetation development (Zhirin et al., 2004; Arkhipova, 2017; Danilova et al., 2017).

Changes in forest cover can lead to changes in the spectral response of the land site (Marchukov, 2010; Potapov et al., 2011; Terekhin and Chendev, 2018). A quantitative analysis of these changes can, in turn, be used to study the vegetation cover of SDVs, including a spatiotemporal analysis of the tree-vegetation percentage in these valleys.

To assess changes in forested lands, researchers most often use approaches based on machine-learning algorithms and on spectral-response classifications

(Huang et al., 2002; Zhang et al., 2014; Potapov et al., 2015; Khovratovich et al., 2019). These approaches allow changes in forests to be mapped at different spatial levels. Meanwhile, a study of development of forest communities in treeless spaces as a successional process requires an assessment of the influence of changes in vegetation on their spectral response. This is due to the fact that forest-development processes can have different effects on spectral response in different parts of the spectrum.

Currently, the problem of how to analyze changes in the spectral response of SDVs, i.e., the changes arising from the formation of tree associations within SDVs, largely remains an open question. Despite being a typical element of landscapes, SDVs are not general, universally widespread objects. They manifest themselves most widely in certain regions, which include the Central Russian forest–steppe (Drozdov, 1991). It is, therefore, relevant to investigate the spectral response of SDVs, because this method can allow researchers to approach the study of changes in their vegetation cover at a new level.

The aim of this study was to quantitatively analyze the spectral response of SDVs and its relationship with the percentage of tree vegetation in ravines and to study the regional trends in SDV forest cover in the CCR in recent decades.

To this end, it was planned to perform the following tasks.

— Informational assessment of spectral response in the context of SDV forest-cover analysis.

— Quantitative assessment of the relationship between SDV forest cover and the spectral characteristics that are most closely correlated with this type of forest cover.

— Spatiotemporal spectral-response analysis of the SDV forest cover within the CCR forest–steppe in the late 20th to early 21st centuries.

METHODS

The object of our research was SDVs located within six regions of Russia: the Belgorod, Voronezh, Kursk, Orel, Lipetsk, and Tambov oblasts. The SDVs were selected on the basis of several criteria: (1) availability of modern (2018) and archival (2000–2018) satellite data of ultrahigh spatial resolution for the SDV sites, (2) the absence of traces of artificial forestation in recent decades, and (3) similar humidification conditions for all the objects, i.e., the absence of swamps within the ravines.

The sample was constructed in such a way as to include SDVs from all the oblasts of the CCR, representing different parts of this region, which was necessary to ensure an objective spatial analysis of forest cover in the SDVs. We also sought to select objects with different forest cover. The absence of signs of artificial forestation in the study period was determined by analyzing the 2000–2018 multitemporal satellite data of ultrahigh spatial resolution (1 m/pixel), which were obtained from open-access web services, mainly Google Earth. The same images were used to analyze the actual forest cover of the ravines. The level of detail of the images enabled a reliable analysis of the modern percentage of tree vegetation in the SDVs. As a result, we selected 162 SDVs with a total area of 3879.6 ha (Table 1).

Table 1. Characteristics of SDVs, which are used for analyzing the changes in forest cover and spectral response

Number of objects	Number of objects	Area, ha
Belgorod oblast	31	933.9
Voronezh oblast	28	876.2
Kursk oblast	34	741.0
Lipetsk oblast	28	389.7
Orel oblast	14	405.7
Tambov oblast	27	533.1
Total	162	3879.6

The satellite images were processed in a geoinformation environment using manual digitization so as to construct two vector contours—the boundary contour and the 2018 forest-site contour—for each SDV. These data were used to calculate the area and the current forest-cover percentage of the SDVs.

Spectral-response analysis of the SDVs was carried out in two stages. In the first stage, we assessed how the forest-cover percentage was related with spectral response and identified those spectral characteristics that were informative for the analysis. In the second stage, we studied the relationship between the forest cover and spectral characteristics of the SDVs.

The relationship between the forest cover and spectral response characteristics of the SDVs was assessed in different spectral ranges from the *Landsat* OLI data. For this purpose, we used the *Landsat-8* OLI satellite scene dated August 24, 2018, with Path 177 and Row 024 parameters in the WRS-2 (Worldwide Reference System-2) and the SDVs covered by this scene. The Path and Row parameters identify the location of the *Landsat* images in the WRS-2, which is used to determine their location on the Earth's surface. The satellite scene was selected so that it covered several dozen target objects, i.e., so that the data obtained could explain the relationship between the forest cover and spectral response. August was chosen as the period of research because it was the least cloudy month of the year; therefore, it was easier to compile cloudless image coverage of the region, which could be used for territorial assessments of the spectral response characteristics of the SDVs.

The *Landsat* OLI images were subjected to atmospheric and radiometric correction and converted into dimensionless spectral reflectance values. The spectral reflectance features of the SDVs were studied by analyzing their response in the main spectral ranges, covering the visible and infrared regions.

The reflective characteristics of the SDVs can also be investigated using spectral vegetation indices, i.e., mathematical transformations of the original brightness of the images. However, because of the diversity of vegetation indices, their analysis, as well as analysis of combinations of spectral-response characteristics pertaining to different spectral ranges for assessing the SDV forest cover, requires a separate study. Meanwhile, it should be noted that interpretation of vegetation indices for vegetation assessment in comparison with the spectral reflectance is not always possible, with their application requiring taking into account a larger number of conditions.

Based on the *Landsat* OLI data, we calculated the spectral reflectance of the SDVs in six ranges: blue, green, red, near-infrared (NIR), and SWIR1 and SWIR2 infrared. We carried out an informational assessment of the spectral indicators for analyzing the SDV forest cover using the Pearson (parametric criterion) and Spearman (nonparametric criterion) correlation coefficients. We analyzed these criteria together in order to increase the objectivity of the results obtained. As part of the study, we assessed the average values of the spectral indicators for the various forest-cover gradations and the significance of the differences between the averages.

We assessed the relationship between the SDV forest cover and spectral response (the second stage of the study) on the basis of the *Landsat* TM/OLI data.

Since the spectral ranges of the *Landsat* TM/ETM+ and *Landsat* OLI sensors are slightly different, we calculated two types of models that describe the relationship between the forest cover and spectral reflectance. The first one uses spectral-response characteristics retrieved from the *Landsat* TM/ETM+ data, and the second one uses those from the *Landsat* OLI data. The analysis of the SDV spectral response using different sensors, albeit with similar characteristics, was aimed at increasing the efficiency of forest-cover modeling in different time sections, which was carried out at the final stage of the study.

The analysis of the relationship between the SDV forest cover and *Landsat* OLI spectral characteristics used the same satellite image (*Landsat-8* of August 24, 2018), which was previously used to investigate the tightness of the relationship between the reflectance and the SDV forest cover. A similar study for the *Landsat* TM spectral characteristics was based on the *Landsat* data of the early 2000s. To this end, we formed a group of SDVs for which we were able to select images of ultrahigh spatial resolution for these periods and to assess the actual forest cover. After that, we used the *Landsat* TM data of August 2000 to assess the relationship between the SDV forest cover and reflectance.

At the final stage, we used the spectral response characteristics identified as the most informative ones for assessing the SDV forest cover to conduct a spatial analysis of forest cover in the mid-1980s, in the early 2000s, and in 2018. To this end, for each time section, we combined the *Landsat* satellite image coverage of the CCR (Table 2).

To minimize the phenological differences, we sought to select satellite images for the same periods of the growing season—mainly August, as it is the least cloudy month. In all the time sections, we were able to pool a sample of relatively cloudless images for this month only. All the images were subjected to atmospheric and radiometric correction and converted to dimensionless reflectance values. The spectral characteristics for specific ravines were calculated using the zonal statistics method; i.e., for each SDV, we calculated a spectral-response value averaged within their contours.

Using the relationships between the SDV forest cover and the SWIR-range reflectance, we estimated the proportion of tree vegetation in each ravine for each of the three time sections: mid-1980s, early 2000s, and 2018. After that, we applied spatial interpolation methods (radial basis functions) to draw schematic maps of the spatial distribution of the SDV forest cover within the CCR for all the time intervals under study. Based on the calculated schematic maps, we identified and investigated the spatiotemporal features of the SDV forest cover in the region at the end of the 20th and beginning of the 21st centuries. The analysis was carried out by assessing the spatial change of territories corresponding to the same SDV forest cover gradations at the beginning and end of the analyzed period.

RESULTS AND DISCUSSION

Based on the estimates, we found that the SDV forest cover is most tightly correlated with the *Landsat-8* OLI SWIR1-range (1.56–1.66 μm) reflectance (Table 3). At the same time, most of the spectral response characteristics are inversely related to the percentage of tree coverage in the SDVs. All the correlations are statistically significant at the 0.05 level, except for the NIR-range reflectance.

Since the SWIR1-range (1.56–1.66 μm) spectral features showed the highest correlation with the SDV forest cover, we used them in a more detailed analysis and spatiotemporal assessment of the SDV spectral response, which served as a basis for the forest cover models.

Statistical analysis of the average values of the reflectance in the 1.56–1.66 μm range for different forest-cover gradations (0–20, 20–40, 40–60, 60–80, and 80–100%) showed that the spectral reflectance values decrease significantly when passing from one gradation to another in the direction of increasing for-

Table 2. *Landsat* satellite data used to assess the spectral response of the SDVs and their forest-cover percentage

Path/Row	Sensor	Record date	Path/Row	Sensor	Record date
177/025	TM TM OLI	Aug. 29, 1985 Aug. 22, 2000 Aug. 24, 2018	174/024	TM ETM+ OLI	July 26, 1986 Aug. 12, 2001 Aug. 19, 2018
175/025	TM TM OLI	Aug. 23, 1988 Aug. 8, 2000 Aug. 26, 2018	179/023	TM TM OLI	Aug. 30, 1986 July 22, 2001 Aug. 6, 2018
179/024	TM TM OLI	Aug. 30, 1986 Sep. 3, 1999 Aug. 6, 2018	177/023	TM TM OLI	Aug. 29, 1985 Aug. 22, 2000 Aug. 24, 2018
178/024	TM ETM+ OLI	Aug. 7, 1986 Sep. 4, 1999 Aug. 31, 2018	176/023	TM TM OLI	Aug. 22, 1988 Sep. 6, 1999 Aug. 1, 2018
177/024	TM TM OLI	Aug. 29, 1985 Aug. 22, 2000 Aug. 24, 2018	175/023	TM ETM+ OLI	July 22, 1988 July 18, 2001 Aug. 26, 2018

Table 3. Tightness of the correlation between the SDV forest-cover percentage and their spectral response (*Landsat-8* OLI)

Correlation coefficient	Spectral reflectance					
	Blue	Green	Red	NIR	SWIR1	SWIR2
Pearson	–0.61	–0.46	–0.41	0.02	–0.79	–0.40
Spearman	–0.52	–0.41	–0.41	0.25	–0.74	–0.48

Table 4. Characteristics of the reflectance in the 1.56–1.66 μm range (*Landsat-8* OLI) for different SDV forest-cover gradations

Forest cover, %	Number of objects	Average	Standard deviation	Minimum	Maximum
0–20	10	0.224	0.013	0.205	0.248
20–40	55	0.200	0.017	0.170	0.239
40–60	52	0.186	0.014	0.159	0.214
60–80	30	0.174	0.018	0.140	0.215
80–100	6	0.166	0.021	0.136	0.188

est-cover percentage (Table 4). The standard deviations revealed no dynamics.

Different models describing the relationship between the SDV forest cover and the *Landsat-8* OLI SWIR-range reflectance were compared in terms of effectiveness to show that the logit function has the highest determination coefficients (R^2) (Table 5, Fig. 1), which indicates that the reflectance values change with different intensities as the forest cover increases. The level of significance of all the equations in Table 5 is less than 0.05.

Similar dependences obtained from the *Landsat* TM data were characterized by slightly lower determination coefficients: 0.52 for the logarithmic model, 0.53 for the power-function model, and 0.55 for the logit function, all at a significance level of 0.05.

The lower determination coefficients for the equations obtained from *Landsat* TM of 2000 are largely due to the absence of ravines with a forest-cover percentage above 60% in the analytical sample for this time interval. The reason for this is that, in the early 2000s, the SDV forest cover was significantly less than today; therefore, we could not find ravines with an appropriate forest-cover percentage. Moreover, the lower values of the determination coefficients may also be due to the lower radiometric resolution of *Landsat* TM in comparison with *Landsat* OLI.

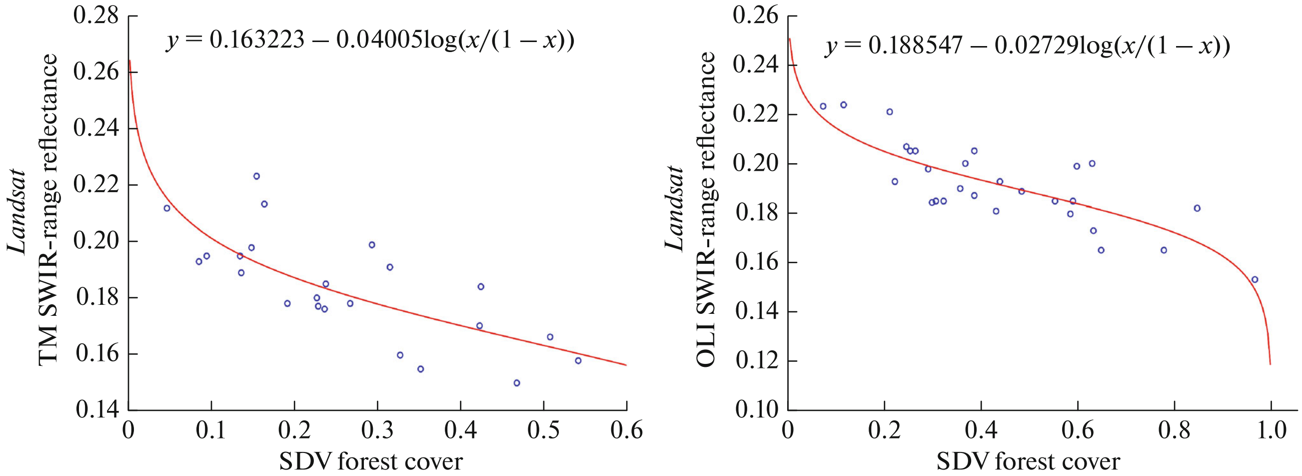

Fig. 1. Curves characterizing the relationship between the SDV forest cover and the SWIR-range spectral reflectance.

It follows from the form of the relationship between the reflectance on the SDV forest cover that the inverse problem, i.e., the problem of assessing the forest cover on the basis of the SWIR-range reflectance, can be solved through the use of a decreasing logistic (sigmoid) curve with asymptotes of 0 and 1 (the minimum and maximum possible forest cover).

Based on the actual SDV forest-cover data and SWIR-range reflectance, the calculated relationship used for assessing the forest cover from *Landsat* OLI data was as follows:

$$y = 1 - \frac{1}{1 + e^{(-44.715x\,+\,8.275)}}, \quad (1)$$

where y are the forest-cover values and x are the values of the SWIR-range reflectance (the sixth band of the *Landsat* OLI sensor). The determination coefficient (R^2) of Eq. (1) was 0.61 at a significance level of 0.05.

A similar relationship based on the *Landsat* TM/ETM+ data was

$$y = 1 - \frac{1}{1 + e^{(-31.342x\,+\,4.639)}}, \quad (2)$$

where y are the forest-cover values and x are the values of the SWIR-range reflectance (the fifth band of the *Landsat* TM/ETM+ sensor). Its determination coefficient (R^2) was 0.60 at a significance level of 0.05. Both (1) and (2) use the SWIR-range reflectance measured in August, which must be taken into account when using these equations.

The use of the proposed relationships for a direct spectral-response assessment of forest cover will give certain errors due to the variability of the SDV spectral response characteristics. Meanwhile, their verification (based on the 2018 data for ravines located outside the Path 177 Row 24 satellite scene) showed that the correlation coefficient of the actual and calculated forest-cover values was approximately 0.80.

A comparison of the actual SDV forest cover in 2018 estimated from satellite data of ultrahigh spatial resolution and the forest cover measured by the SWIR-range reflectance showed (Table 6) that the actual and calculated values virtually coincide for the CCR as a whole and in most oblasts of the CCR.

In Belgorod, Lipetsk, and Orel oblasts, the calculated values of the SDV forest cover are virtually no different from the actual ones. In Voronezh, Kursk, and Tambov oblasts, the deviations are more significant, perhaps due to the use (since there are no data for other dates) for considerable land areas of *Landsat* OLI images taken in early August, rather in the second half of this month, like those used to calculate the equation and estimate the forest-cover percentage in most of the study area.

Table 5. Characteristics of the dependences describing the relationship between the SDV forest cover and SWIR-range reflectance values (*Landsat-8* OLI)

Type of dependence	Equation	R^2
Linear	$y = -0.0613x + 0.2184$	0.62
Logarithmic	$y = -0.024\ln(x) + 0.1688$	0.64
Power function	$y = 0.1695x^{-0.123}$	0.63
Logit function	$y = 0.1885 - 0.0273\log(x/(1-x))$	0.65

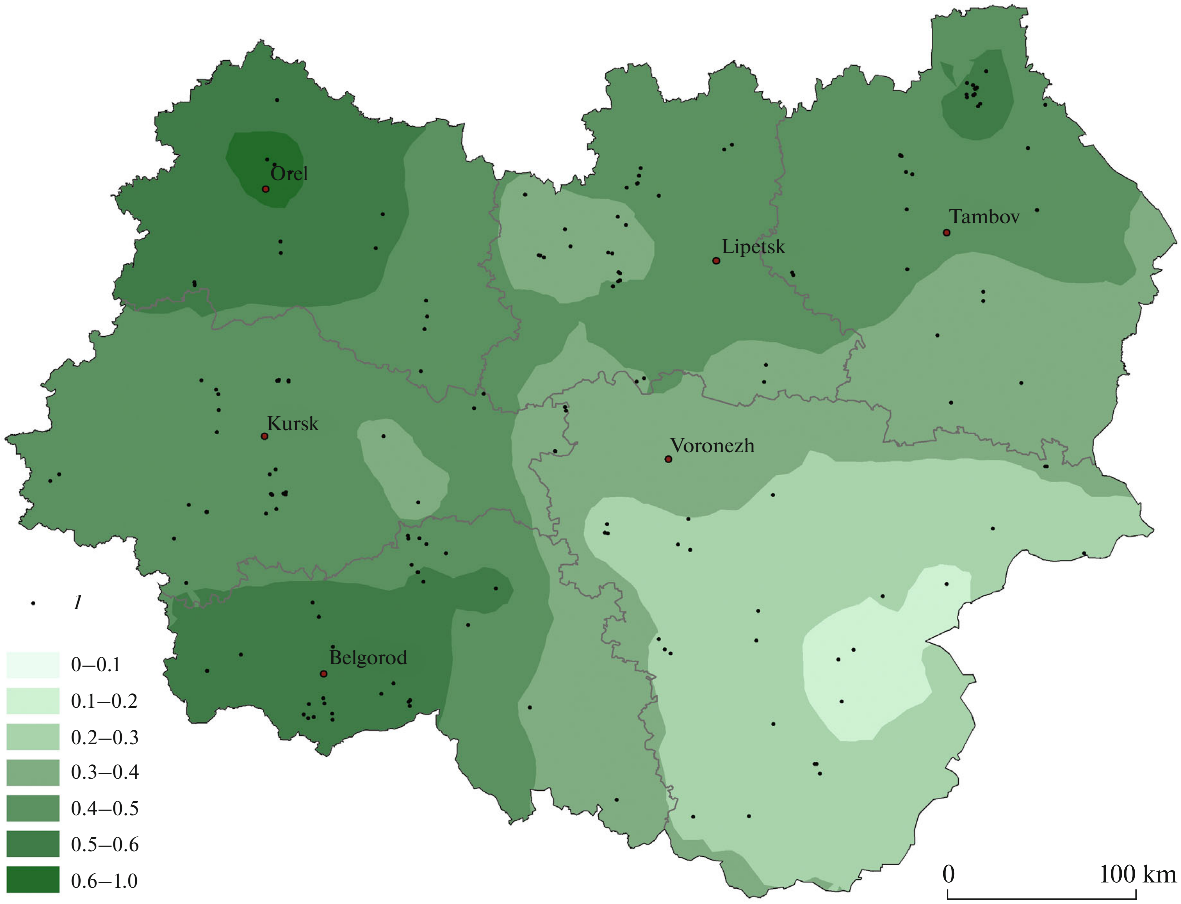

Fig. 2. Spatial change in the SDV forest cover within the CCR (2018) modeled from the *Landsat-8* OLI SWIR-range spectral response. (*1*) The studied SDVs.

The presence of a statistically significant relationship between the SDV forest cover and the SWIR-range reflectance provided a basis for conducting a spatiotemporal spectral-response analysis of this relationship within the CCR forest–steppe in 1985–2018.

The territorial analysis of the modern (2018) forest-cover percentage calculated from the SWIR-range reflectance (Fig. 2), made it possible to identify its features. We drew up a schematic map by the spatial-interpolation method (radial basis functions (RBFs)) using the capabilities of geographic information systems.

The key territorial patterns of the change in forest cover that are visible in the schematic map can be formulated as follows.

(1) Sufficiently high differences in the modern SDV forest cover within the region.

Table 6. Comparison of the actual SDV forest cover with the results calculated from the SWIR-range reflectance for different oblasts of the CCR

Region	SDV forest cover in 2018			
	actual		calculated	
	average	standard deviation	average	standard deviation
Belgorod oblast	0.55	0.20	0.54	0.15
Voronezh oblast	0.28	0.14	0.21	0.12
Kursk oblast	0.49	0.17	0.41	0.15
Lipetsk oblast	0.42	0.13	0.40	0.15
Orel oblast	0.59	0.13	0.61	0.15
Tambov oblast	0.39	0.16	0.52	0.17
CCR average	0.45	0.18	0.44	0.18

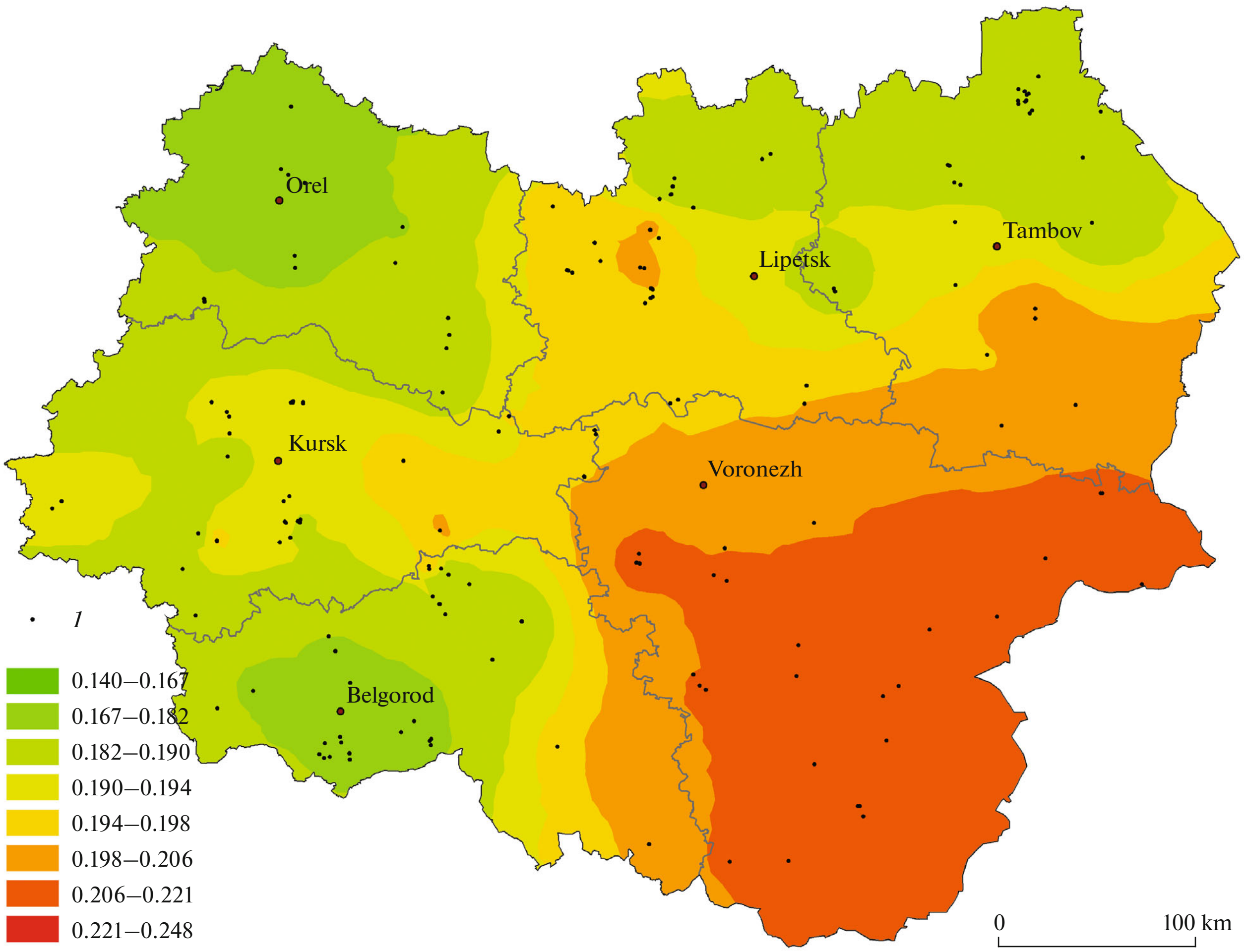

Fig. 3. Spatial distribution of the SWIR-range reflectance for SDVs within the CCR in 2018. (*1*) The studied SDVs.

(2) The presence of spatial trends in the change in forest cover within the CCR. A decrease in the SDV forest cover is observed in two main directions: from northwest to southeast and from northeast to southwest. At the same time, in the south of the CCR, significant differences are observed between the western and eastern parts.

The substantial modern territorial differences in the SDV forest cover are due to the different natural and climatic conditions, which enable a more or less intense growth of tree vegetation in valleys and ravines. They change in going from the forest-zone and northern-forest–steppe-subzone conditions in the northwest and northeast to the steppe conditions in the southeast (*Fiziko-geograficheskoe raionirovanie*, 1961).

Since the SDV forest cover and the SWIR-range reflectance values show a rather high correlation ($R = -0.79$), the assessment of territorial changes in the forest cover can also be performed directly by conducting a spatial analysis of these spectral characteris-

Table 7. Parameters of the change in the forest cover of SDVs in the CCR forest–steppe from the late 20th to early 21st centuries

Year	SDV forest cover			
	average	minimum	maximum	stand. dev.
1985	0.16	0.03	0.43	0.08
2000	0.26	0.04	0.49	0.09
2018	0.45	0.04	0.90	0.20

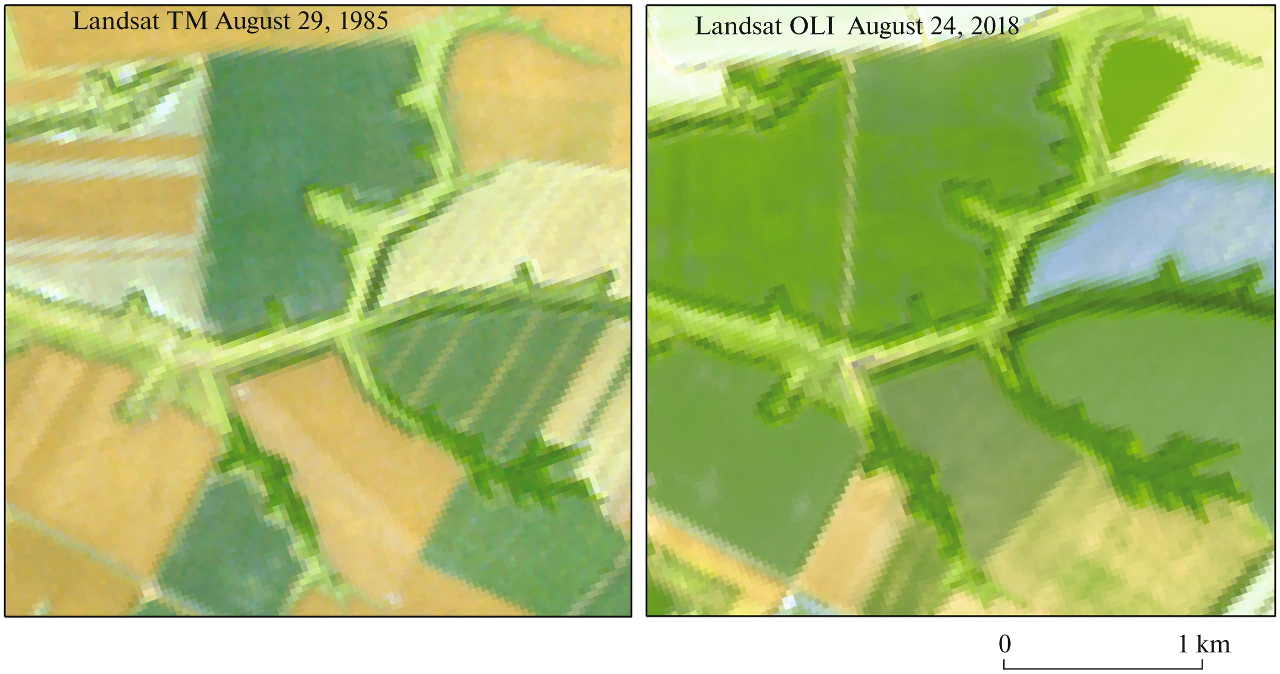

Fig. 4. An example showing the change in the SDV forest-cover percentage in 1985–2018 across the Central Russian forest–steppe. Belgorod oblast.

tics. The territorial assessment of the reflectance values measured in 2018 showed that the parameters of their change (Fig. 3) are in many respects similar to the spatial features of the SDV forest cover in the same year (Fig. 2), except that the growth of the forest cover was accompanied by a decrease in the reflectance.

For example, one can clearly trace differences in the SDV forest cover between the southwestern and southeastern parts of the region, which were identified from the SDV forest cover data and from the reflectance. Thus, a direct analysis of the spatiotemporal characteristics of the SWIR-range spectral response can give an idea of the territorial change in the SDV forest cover.

The results of modeling the CCR SDV forest cover using the SWIR-range reflectance showed that over the past decades, from the mid-1980s to 2018, a significant, almost threefold increase in the SDV forest cover was observed within the CCR forest–steppe zone (Table 7).

Simultaneously, an increase was observed in its maximum, minimum, and standard deviation, which indicates that the modern appearance of the SDVs is now more diverse in terms of forest cover than 30–35 years ago. The changes in all the indicators of the SDV forest cover occurred sequentially. In 1985–2000, the SDV forest cover increased from 16 to 26%, i.e., by a factor of 1.6. In 2000–2018, it increased from 26 to 45%, i.e., by a factor of 1.7. In total, the SDV forest cover increased over the 33 years, according to the data obtained, by a factor of 2.8. The increased differences in the forest cover may result from the increased contrasts in the natural and climatic conditions, which, in turn, are prone to variations.

The results obtained are confirmed by a visual analysis of the SDV forest cover in the mid-1980s and in 2018 (Fig. 4) from the satellite data. Since the spatial resolution of the *Landsat* images is not very high (30 m/pixel), we could not use them to obtain quantitative estimates for the forest-cover percentage in the same way as we did with the ultrahigh spatial resolution images of 2018. Nevertheless, the increasing tendency in the forest cover manifests itself quite clearly in these images when the same ravine sites are compared. It is seen from Fig. 4 that, in the period under study, the increase in the SDV forest cover was due to an increase in the area covered by forests both in the upper reaches of the ravines and on their slopes and central parts.

Thus, at the turn of the 20th and 21st centuries, over at least the last four decades, an ongoing natural growth has been observed of the SDV forest cover on the territory of the CCR forest steppe. This growth results in a change in the landscape appearance of the SDVs due to the transformation of grassy spaces into forest ecosystems.

CONCLUSIONS

The changes in the forest cover of small dry valleys (SDVs) affect their spectral response. Having analyzed the forest cover of SDVs typical of the Central

Russian forest–steppe, we found the SWIR-range (1.56–1.66 μm) reflectance values to be the most informative ones in the visible and infrared ranges for analyzing the proportion of tree vegetation in the SDVs. An increase in forest-cover percentage is accompanied by a decrease in the SWIR-range spectral reflectance. A forest-cover assessment based on SWIR-range spectral response can be performed using a logistical curve. Using the spectral response measured from the data obtained from the *Landsat* sensors, we carried out a spatiotemporal assessment of the SDV forest cover for the forest steppe in the Central Chernozem region of Russia in 1985–2018. The increase in the SDV forest-cover percentage was confirmed. During the study period, it increased from 16 to 45%. At present, significant differences are observed within the region in the forest cover of ravine systems, unlike in the mid-1980s, when no such patterns were recorded. These differences may be due to an increase in natural and climatic contrasts across the region.

CONFLICT OF INTEREST

The author declares that he has no conflicts of interest.

REFERENCES

Arkhipova, M.V., Reafforestation of disturbed lands in the Ugra national park, *Vestn. Mosk. Univ., Ser. 5: Geogr.*, 2017, no. 1, pp. 92–99.

Belyaeva, N.G. and Popov, S.Yu., Change in the forest coverage of the former Vereya district of the Moscow region over 200 years, *Lesovedenie*, 2016, no. 1, pp. 44–54.

Bonan, G.B., Forests and climate change: Forcings, feedbacks, and the climate benefits of forests, *Science*, 2008, vol. 320, no. 5882, pp. 1444–1449. https://doi.org/10.1126/science.1155121

Bugaev, V.A., Revin, A.I., and Musievskii, A.L., Dynamics of the forest resources in the Central Black Earth region, *Les. Khoz.*, 2006, no. 3, pp. 41–42.

Chendev, Yu.G., Hubbart, J.A., Terekhin, E.A., Lupo, A.R., Sauer, T.J., and Burras, C.L., Recent afforestation in the Iowa River and Vorskla River basins: A comparative trends analysis, *Forests*, 2016, vol. 7, no. 11. https://doi.org/10.3390/f7110278

Danilova, I.V., Korets, M.A., and Ryzhkova, V.A., Mapping age stages of forest vegetation based on an analysis of Landsat multiseasonal satellite images, *Izv., Atmos. Ocean. Phys.*, 2017, vol. 54, no. 9. 997–1007.

Drozdov, K.A., *Elementarnye landshafty srednerusskoi lesostepi* (Elementary Landscapes of the Middle Russian Forest Steppe), Voronezh: VGU, 1991.

Fiziko-geograficheskoe raionirovanie tsentral'nykh chernozemnykh oblastey (Physico-Geographical Zoning of the Central Chernozem Regions), Voronezh: Izd. Voronezh. Univ., 1961.

Gao, J. and Liu, Y., De(re)forestation and climate warming in subarctic China, *Appl. Geogr.*, 2012, vol. 32, pp. 281–290. https://doi.org/10.1016/j.apgeog.2011.04.002

Huang, C., Davis, L.S., and Townshend, J.R.G., An assessment of support vector machines for land cover classification, *Int. J. Remote Sens.*, 2002, vol. 23, no. 4, pp. 725–749. https://doi.org/10.1080/01431160110040323

Kashnitskii, A.V., Khovratovich, T.S., and Balashov, I.V., The organization of remote sensing data processing for solving the problems of deforestation detection in large areas, *Sovrem. Probl. Distantsionnogo Zondirovaniya Zemli Kosmosa*, 2019, vol. 16, no. 6, pp. 103–111.

Khovratovich, T.S., Bartalev, S.A., and Kashnitskii, A.V., A method for detecting forest changes based on a subpixel estimate of the projective cover of the tree canopy from multi-temporal satellite images, *Sovrem. Probl. Distantsionnogo Zondirovaniya Zemli Kosmosa*, 2019, vol. 16, no. 4, pp. 102–110. https://doi.org/10.21046/2070-7401-2019-16-4-102-110

Kim, D.-H., Sexton, J.O., Noojipady, P., Huang, C., Anand, A., Channan, S., Feng, M., and Townshend, J.R., Global, Landsat-based forest-cover change from 1990 to 2000, *Remote Sens. Environ.*, 2014, vol. 155, pp. 178–193. https://doi.org/10.1016/j.rse.2014.08.017

Kozoderov, V.V., Donskoi, S.A., Mel'nik, P.G., and Dmitriev, E.V., Evaluation of the Species Composition and the Biological Productivity of Forests Based on Remote Sensing Data with High Spatial and Spectral Resolution, *Izv., Atmos. Ocean. Phys.*, 2018, vol. 54, no. 9, pp. 1374–1380.

Lebedeva, M.G. and Krymskaya, O.V., Manifestation of current climate changes in the Belgorod region, *Nauchn. Vedomosti Belgorod. Gos. Univ., Ser. Estestv. Nauki*, 2008, vol. 3, no. 6, pp. 188–196.

Marchukov, V.S., Automated methods for assessing the dynamics of spatial distribution of vegetation cover and soils from remote sensing data, *Issled. Zemli Kosmosa*, 2010, no. 2, pp. 63–74.

Mil'kov, F.N., Akhtyrtseva, N.I., Drozdov, K.A., Khmelev, K.F., Dvurechenskii, V.N., Drozdov, K.A., Mikhno, V.B., Akhtyrtsev, B.P., Skuf'in, K.V., Grigor'evskaya, A.Ya., and Fedotov, V.I., *Izvestnyakovyi sever Srednerusskoi vozvyshennosti* (The Limestone North of the Middle Russian Upland), Voronezh, 1978.

Nechetova, Yu.V. and Narozhnyaya, A.G., Study of the ravine-gully network of the Belgorod region using GIS technologies, *Zemleustroistvo Kadastr Monit. Zemel*, 2010, no. 11, pp. 96–100.

Novikova, E.P., Grigor'ev, G.N., Vagurin, I.Yu., and Chumeikina, A.S., Variations in the hydrothermal regime in the Black Earth region over the past 30 years against the background of global climate change, *Nauchn. Vedomosti Belgorod. Gos. Univ., Ser. Estestv. Nauki*, 2017, vol. 39, no. 11, pp. 105–113.

Ol'chev, A.V., Rozinkina, I.A., Kuz'mina, E.V., Nikitin, M.A., and Rivin, G.S., Assessment of the impact of changes in the forest coverage of the central region of the East

European Plain on summer weather conditions, *Fundam. Prikl. Klimatol.*, 2017, vol. 4, pp. 83–105.

Onuchin, A.A., Gaparov, K.K., and Mikheeva, N.A., Influence of forest coverage and climatic factors on the annual flow of rivers in the Issyk-Kul region, *Lesovedenie*, 2008, no. 6, pp. 45–52.

Pis'man, T.I., Botvich, I.Yu., and Shevyrnogov, A.P., Assessment of the state of forests in the Krasnoyarsk region (the *Stolby reserve*) according to satellite data, *Sovrem. Probl. Distantsionnogo Zondirovaniya Zemli Kosmosa*, 2018, vol. 15, no. 5, pp. 130–140.

Potapov, P., Turubanova, S., and Hansen, M.C., Regional-scale boreal forest cover and change mapping using Landsat data composites for European Russia, *Remote Sens. Environ.*, 2011, vol. 115, no. 2, pp. 548–561. https://doi.org/10.1016/j.rse.2010.10.001

Potapov, P.V., Turubanova, S.A., Tyukavina, A., Krylov, A.M., McCartyb, J.L., Radeloff, V.C., and Hansen, M.C., Europe's forest cover dynamics from 1985 to 2012 quantified from the full Landsat archive, *Remote Sens. Environ.*, 2015, vol. 159, pp. 28–43. https://doi.org/10.1016/j.rse.2014.11.027

Terekhin, E.A., Assessment of forest disturbance in the forest–steppe zone in the early 21st century according to satellite data, *Sovrem. Probl. Distantsionnogo Zondirovaniya Zemli Kosmosa*, 2020, vol. 17, no. 2, pp. 134–146.

Terekhin, E.A. and Chendev, Yu.G., Estimation of forest cover changes during modern period in the south of the Central Russian Upland using multiyear remote sensing data, *Sovrem. Probl. Distantsionnogo Zondirovaniya Zemli Kosmosa*, 2018, vol. 15, no. 3, pp. 114–126.

Zhang, J., Pham, T.-T.-H., Kalacska M., and Turner, S., Using Landsat Thematic Mapper records to map land cover change and the impacts of reforestation programmes in the borderlands of southeast Yunnan, China: 1990–2010, *Int. J. Appl. Earth Obs. Geoinf.*, 2014, vol. 31, pp. 25–36. https://doi.org/10.1016/j.jag.2014.01.006

Zhirin, V.M., Sukhikh, V.I., Shatalov, A.V., Butusov, O.B., and Eidlina, S.P., Satellite images for studying the dynamics of overgrowing of burnt areas, *Issled. Zemli Kosmosa*, 2004, no. 5, pp. 69–76.

Translated by A. Kobkova